

Internal Conductance to CO₂ Diffusion and C¹⁸O₂ Discrimination in C₃ Leaves¹

Jim S. Gillon and Dan Yakir*

Department of Environmental Science and Energy Research, Weizmann Institute of Science, 76100 Rehovot, Israel

¹⁸O discrimination in CO₂ stems from the oxygen exchange between ¹⁸O-enriched water and CO₂ in the chloroplast, a process catalyzed by carbonic anhydrase (CA). A proportion of this ¹⁸O-labeled CO₂ escapes back to the atmosphere, resulting in an effective discrimination against C¹⁸O₂ during photosynthesis ($\Delta^{18}\text{O}$). By constraining the $\delta^{18}\text{O}$ of chloroplast water (δ_e) by analysis of transpired water and the extent of CO₂-H₂O isotopic equilibrium (θ_{eq}) by measurements of CA activity ($\theta_{\text{eq}} = 0.75\text{--}1.0$ for tobacco, soybean, and oak), we could apply measured $\Delta^{18}\text{O}$ in a leaf cuvette attached to a mass spectrometer to derive the CO₂ concentration at the physical limit of CA activity, i.e. the chloroplast surface (c_{cs}). From the CO₂ drawdown sequence between stomatal cavities from gas exchange (c_i), from $\Delta^{18}\text{O}$ (c_{cs}), and at Rubisco sites from $\Delta^{13}\text{C}$ (c_c), the internal CO₂ conductance (g_i) was partitioned into cell wall (g_w) and chloroplast (g_{ch}) components. The results indicated that g_{ch} is variable ($0.42\text{--}1.13 \text{ mol m}^{-2} \text{ s}^{-1}$) and proportional to CA activity. We suggest that the influence of CA activity on the CO₂ assimilation rate should be important mainly in plants with low internal conductances.

Natural variation in ¹⁸O content ($\delta^{18}\text{O}$) of CO₂ is a useful tracer for photosynthetic activity. This is due to a sequence of events: first, $\delta^{18}\text{O}$ of chloroplast water is high due to evaporative effects (Gonfiatini et al., 1965); second, in the chloroplasts, exchange of oxygen between CO₂ and H₂O is catalyzed by carbonic anhydrase (CA); and third, a large fraction of this ¹⁸O-labeled CO₂ diffuses from the chloroplast back to the atmosphere. On a leaf scale, this "retroflux" of ¹⁸O-enriched CO₂ from the leaf back to the atmosphere is observed as an enrichment in the C¹⁸O₂ in air passing over the leaf or as discrimination against C¹⁸O₂ by the leaf ($\Delta^{18}\text{O}$) (Farquhar and Lloyd, 1993). Notably, $\Delta^{18}\text{O}$ is also observed on a global scale as latitudinal and seasonal changes in the $\delta^{18}\text{O}$ of atmospheric CO₂. The quantitative use of such large-scale signals, however, still critically depends on better understanding of the basic processes influencing $\Delta^{18}\text{O}$ (Francey and Tans, 1987; Farquhar et al., 1993; Ciais et al., 1997).

To interpret $\Delta^{18}\text{O}$ measured during leaf-atmosphere CO₂ exchange, an estimate of CO₂ concentration at the site of CO₂-H₂O is required (Farquhar and Lloyd, 1993). The chloroplast CO₂ concentration (c_c) may be derived from comparing measured and modeled discrimination against ¹³CO₂ ($\Delta^{13}\text{C}$) (Farquhar et al.,

1982; Evans et al., 1986; von Caemmerer and Evans, 1991). Since both the photosynthetic enzyme Rubisco (responsible for ¹³C discrimination) and CA (responsible for $\Delta^{18}\text{O}$) are similarly distributed within the chloroplast stroma (Anderson et al., 1996), the ¹³C-derived value of c_c was also applied to $\Delta^{18}\text{O}$ (Farquhar et al., 1993; Flanagan et al., 1994). However, it was suggested (Yakir, 1998) that the CO₂ concentration pertaining to $\Delta^{18}\text{O}$ may be associated with the chloroplast surface, i.e. the limit of CA activity, and not the mean CO₂ concentration at sites of CO₂ fixation by Rubisco. This is because CA acts to cancel out any gradients in ¹⁸O of CO₂ within its domain. We now suggest that with adequate estimates of chloroplast water $\delta^{18}\text{O}$ and of the extent of CO₂-H₂O isotopic equilibrium in the chloroplast (i.e. CA activity), it should be possible to use $\Delta^{18}\text{O}$ to accurately estimate the effective CO₂ concentration at the sites of CO₂-H₂O equilibrium. This approach is somewhat similar to that using observed and predicted $\Delta^{13}\text{C}$ to compare c_i and c_c (von Caemmerer and Evans, 1991).

Using ¹³C-derived estimates of c_c , the internal leaf conductance to CO₂ (g_i) and its influence on leaf photosynthesis have been well characterized (von Caemmerer and Evans, 1991; Lloyd et al., 1992; Loreto et al., 1992; Syvertsen et al., 1995). However, evaluating the relative importance of the major components of g_i , the wall conductance (g_w) and the chloroplast conductance (g_{ch}) has been restricted (Cowan, 1986; Evans et al., 1994). The association of $\Delta^{18}\text{O}$ with CO₂ concentration at the chloroplast surface should enable this partitioning. Information on CA activity directly from assays or through $\Delta^{18}\text{O}$ measurements should also provide insight into the role of CA in facilitating diffusion within the chloro-

¹ This research was supported by the Israel Science Foundation (grant no. 308/96). J.S.G. was supported by a fellowship from the Leverhulme Trust, UK (no. SAS/30317) while at the Weizmann Institute of Science, and by the Natural Environment Research Council, UK (grant no. GT4/94/379) while at University of Newcastle upon Tyne, Department of Agriculture and Environmental Sciences, Ridley Building, Newcastle upon Tyne, UK.

* Corresponding author; e-mail ciyakir@wisemail.weizmann.ac.il; fax 972-8-934-4124.

plast (Cowan, 1986; Makino et al., 1992; Price et al., 1994; Williams et al., 1996).

By comparing the CO₂ concentration and isotopic composition of air entering and leaving a leaf chamber, discrimination against C¹⁸O (Δ¹⁸O) may be measured "on-line" in a method equivalent to Δ¹³C (Evans et al., 1986):

$$\Delta = \frac{\xi(\delta_0 - \delta_{in})}{1,000 + \delta_0 - \xi(\delta_0 - \delta_{in})} \cdot 1,000 \quad (1)$$

where $\xi = c_{in}/(c_{in}-c_o)$, c_{in} , c_o , and δ_{in} , δ_o referring to the CO₂ concentration (corrected to the same humidity) and isotopic composition of air entering and leaving the cuvette, respectively. Δ¹⁸O can also be predicted (Farquhar and Lloyd, 1993) as

$$\Delta^{18}\text{O} = \frac{\bar{a} + \epsilon\Delta_{ea}}{1 - \epsilon\Delta_{ea}/1,000} \quad (2)$$

where $\Delta_{ea} = 1,000 \cdot [(\delta_e/1,000 + 1)/(\delta_a/1,000 + 1) - 1]$; $\epsilon = c_c/(c_a - c_c)$; δ_a and δ_e represent the δ¹⁸O of CO₂ in the overlying air and in full isotopic equilibrium with water in the chloroplast, respectively, and c_a and c_c the respective CO₂ concentrations (see Fig. 1); \bar{a} is the weighted-mean diffusional fractionation through the boundary layer, 5.8‰, stomata, 8.8‰, and aqueous leaf media, 0.8‰, (Farquhar and Lloyd, 1993). Despite general agreement between modeled and measured Δ¹⁸O (Farquhar et al., 1993; Flanagan et al., 1994; Williams et al., 1996), large quantitative discrepancies often occur (Yakir et al., 1994; Williams et al., 1996; Harwood et al., 1998; Wang et al., 1998). There are three main assumptions in Equation 2: (a) chloroplast water (and hence CO₂ in equilibrium with this water) is assumed to be isotopically similar to water at the evaporating sites (δ_e); (b) CO₂ and H₂O in the chloroplast reach full isotopic equilibrium; and (c) c_c correctly represents the CO₂ concentration at the site of oxygen exchange.

The isotopic composition of water at evaporating surfaces (δ_e) may be estimated from the Craig and Gordon model of evaporative enrichment (Craig and Gordon, 1965):

$$\delta_e = \delta_t + \epsilon^* + \epsilon_k + h^* \cdot (\delta_a - \epsilon_k - \delta_t) \quad (3)$$

where h^* is the relative humidity at leaf temperature; δ_a and δ_t are the isotopic composition of water vapor in the air and transpired by the leaf, respectively; ϵ_k is the combined diffusional fractionation through stomata and turbulent boundary layer (Farquhar and Lloyd, 1993; Buhay et al., 1996); and ϵ^* is the temperature-dependent liquid-vapor fractionation. The measurement of δ¹⁸O of transpired water vapor (δ_t) allows estimation of δ_e under non-steady-state conditions (Harwood et al., 1998). While the proximity of chloroplasts to the liquid-air interface in leaves implies good mixing between evaporating sites and chloroplasts, isotopic gradients in leaf water can oc-

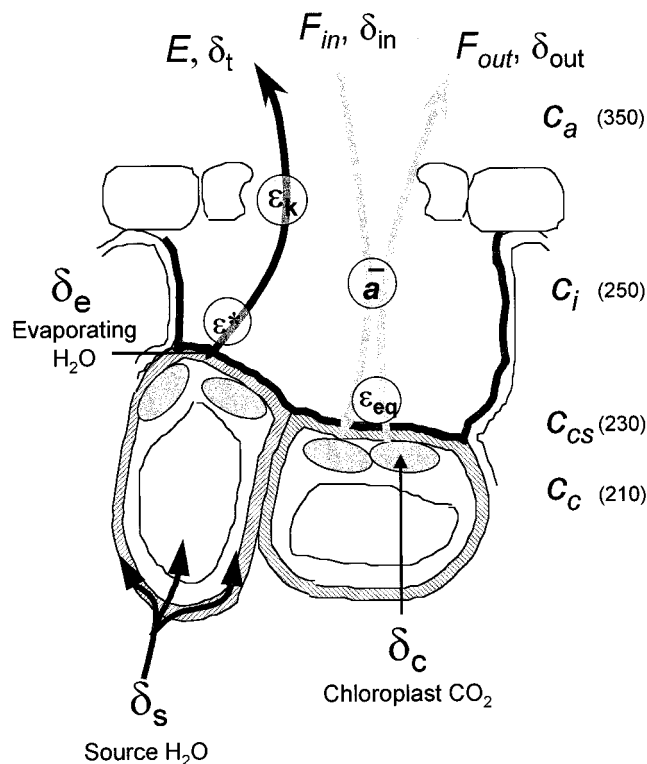


Figure 1. Diagram showing the ¹⁸O content in fluxes of CO₂ (F_{out}) and H₂O (E) from leaf to atmosphere. H₂O enters the leaf with isotopic composition δ_s , evaporates from the cell surfaces, and diffuses from the leaf, experiencing both phase-change (ϵ^*) and diffusional (ϵ_k) fractionation, giving rise to depleted transpiring water (δ_t) and enriched evaporating surfaces (δ_e). Similarly, CO₂ from the atmosphere (F_{in}) dissolves in the chloroplast, equilibrates (ϵ_{eq}) to composition δ_c depending on the δ¹⁸O of water in the chloroplast and the extent of isotopic equilibrium (θ_{eq}), and then approximately two-thirds retro-diffuses outward (F_{out}) with fractionation during diffusion (\bar{a}). This can be observed as an ¹⁸O enrichment in outgoing CO₂ (δ_{out}) relative to incoming CO₂ (δ_{in}), which is proportional to discrimination against C¹⁸O, termed Δ¹⁸O. CO₂ reference points along the leaf-atmosphere pathway are marked (with average values in μmol mol⁻¹) as c_c , c_{cs} , c_i , and c_a , referring to the CO₂ concentration in the chloroplast, chloroplast surface, substomatal cavity, and air, respectively.

cur (Yakir et al., 1989, 1994; Luo and Sternberg, 1992; Wang and Yakir, 1995) and need to be considered.

Considering oxygen isotope exchange between CO₂-H₂O, current estimates have suggested isotopic exchange to be almost complete, approximately 95% (Farquhar and Lloyd, 1993; Flanagan et al., 1994; Williams et al., 1996). However, given the potential uncertainties in δ¹⁸O of water and CO₂ concentration in the chloroplast when interpreting Δ¹⁸O, an independent method is still required to test this assumption. Alternatively, the extent of isotopic equilibrium (θ_{eq}) in the CO₂-H₂O system may be derived from Mills and Urey (1940) as:

$$\theta_{eq} = 1 - e^{-k\tau/3} \quad (4)$$

which describes the fractional approach to full equilibrium (where $\theta_{eq} = 1$) as a function of the number

of hydration reactions achieved per CO₂ molecule ($k\tau$). This “coefficient of CO₂ hydration” may be calculated for a leaf by calculating the rate constant (k) from biochemical measurements of CA activity and the residence time of CO₂ in the leaf (τ) from photosynthetic flux measurements of CO₂ (see “Materials and Methods”). In this way, the extent of isotopic equilibrium may be directly determined.

We sought to determine the CO₂ concentration relevant to CO₂-H₂O in leaves from measurements of $\Delta^{18}\text{O}$ by constraining both the $\delta^{18}\text{O}$ of exchangeable water and the extent of isotopic equilibrium as above. The subsequent implications toward internal CO₂ conductance are discussed in the context of CA activity and its role in facilitating diffusion of CO₂ within the chloroplast.

RESULTS AND DISCUSSION

Interpreting C¹⁸OO discrimination requires information on $\delta^{18}\text{O}$ of water in the chloroplasts, the extent of isotopic equilibrium between CO₂-H₂O and the CO₂ concentration in the chloroplast. The $\delta^{18}\text{O}$ value of chloroplast water is often derived from the Craig and Gordon model for evaporating water (δ_e in Eq. 3; Flanagan et al., 1994; Williams et al., 1996; Yakir and Wang, 1996; Wang et al., 1998; Harwood et al., 1998). This is due to the proximity of chloroplasts to the liquid-air interfaces within leaves. This leaves two options in using Equation 2 and measurements of $\Delta^{18}\text{O}$: (a) to use $\Delta^{13}\text{C}$ -derived estimates of c_c as the CO₂ concentration relevant to the site of oxygen exchange in the chloroplast and solve for the extent of isotopic equilibrium (e.g. Flanagan et al., 1994); and (b) to independently measure the extent of isotopic equilibrium and solve for c_c . We argue that c_c does not refer to the site of CO₂-H₂O equilibrium and so took the latter approach to estimate its true value. Using constrained estimates of δ_e and direct assays of CA activity, we solved both $\Delta^{18}\text{O}$ and $\Delta^{13}\text{C}$ discrimination equations for c_c . We found the $\Delta^{18}\text{O}$ -derived c_c to be always higher than $\Delta^{13}\text{C}$ -derived values, and define the CO₂ concentration relevant to $\Delta^{18}\text{O}$ as c_{cs} (for [CO₂] at the chloroplast surface). We then use c_{cs} to partition the internal conductance into its two major components. In the following sections we show how the interpretations were constrained and discuss their implications.

Observed $\Delta^{18}\text{O}$

Consistent with previous observations and predictions, a clear dependence of $\Delta^{18}\text{O}$ on c_c/c_a was observed (Fig. 2; Farquhar et al., 1993; Flanagan et al., 1994; Williams and Flanagan, 1996; Williams et al., 1996). As expected, $\Delta^{18}\text{O}$ was also larger when measured using ¹⁸O-depleted source CO₂, which generated a larger isotopic difference between source and leaf CO₂ (Δ_{ca}) (increasing the precision of measure-

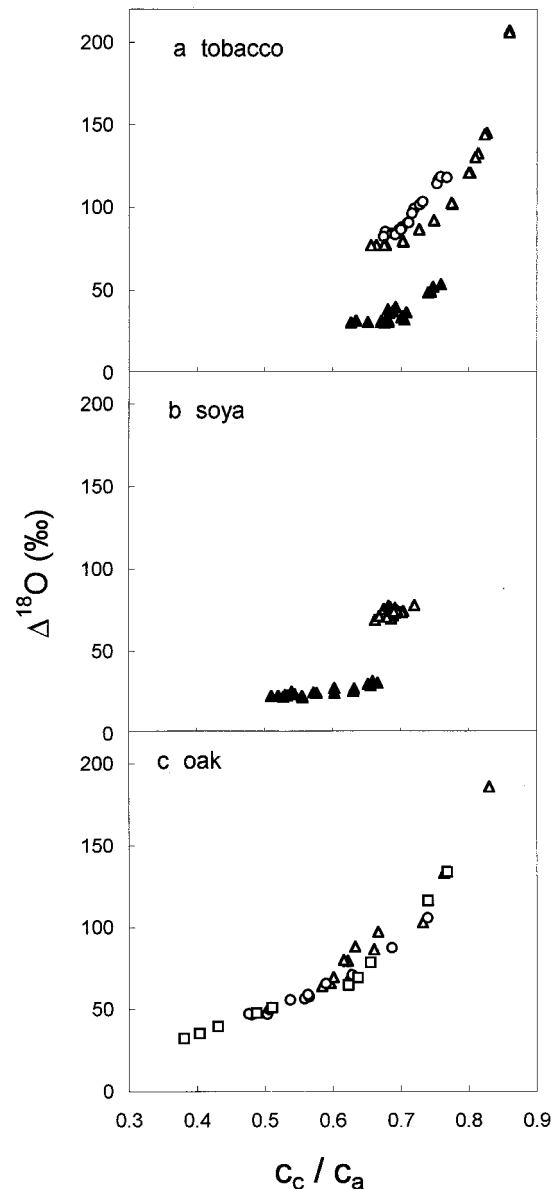


Figure 2. Discrimination against C¹⁸OO ($\Delta^{18}\text{O}$) as a function of chloroplast CO₂ concentration (calculated from $\Delta^{13}\text{C}$) and expressed as c_c/c_a for tobacco (a), soy (b), and oak (c). In a and b, experiments were conducted under depleted source CO₂ (−30‰, white symbols) and ambient CO₂ (0‰, black symbols). For oak, experiments were conducted all in depleted CO₂, but at 2% (squares), 21% (circles), and 35% (triangles) oxygen.

ment). No difference in the response was observed under different photorespiratory conditions in oak leaves (Fig. 2c). Low $p\text{O}_2$ did, however, induce higher assimilation rates and lower c_i and c_c (Table I) due to reduced photorespiration. Estimates of internal CO₂ conductance (g_i) derived from $\Delta^{13}\text{C}$ measurements were 0.50 (± 0.12), 0.32 (± 0.05), and 0.27 (± 0.09) mol m^{−2} s^{−1} for tobacco, soy, and oak respectively, which were used to calculate c_c/c_a . Our g_i estimates were in line with previous estimates on similar herbaceous

Table 1. Gas exchange (at max PPFD), CA activity, and isotopic water data (average at all PPFDs) for tobacco, soy ($n = 3$ and 2), and oak ($n = 3$, at different $O_2\%$)

Units are: evaporation rate (E_{max} , $\text{mmol m}^{-2} \text{s}^{-1}$), stomatal CO_2 conductance ($g_{s(max)}$, $\text{mmol CO}_2 \text{ m}^{-2} \text{ s}^{-1}$), CO_2 assimilation (A_{max} , $\mu\text{mol m}^{-2} \text{ s}^{-1}$), sub-stomatal CO_2 concentration (c_i , $\mu\text{mol mol}^{-1}$), leaf temperature (T_{max} , $^{\circ}\text{C}$), carbonic anhydrase CO_2 hydration rate, under assay (CA_{assay} , at 2°C and $35 \text{ mM } [\text{CO}_2]$, mean of three leaves), and in vivo conditions (CA_{leaf} at c_{cs} and T_{leaf} , $\mu\text{mol CO}_2 \text{ m}^{-2} \text{ s}^{-1}$). For VPD (kPa) and isotopic data (‰), nos. are averages (+SD) during the entire light response. Symbols as in text.

Species	E_{max}	$g_{s(max)}$	A_{max}	$c_{i(min)}$	T_{max}	CA_{assay}	CA_{leaf}	VPD	δ_t	δ_e	δ_{LW}
							$\times 10^3$				
Tobacco 1	5.5	244	14.1	274	27.2	n.d.	1,623 ^a	1.37 (0.19)	-6.3(0.9)	+12.0(1.1)	+11.0
Tobacco 2	4.8	189	13.5	240	29.3	54.8(13)	598	1.48 (0.17)	-5.5(0.6)	+15.6(1.0)	+11.9
Tobacco 3	5.0	241	15.8	265	28.5	71.3(6.3)	670	1.27 (0.18)	-2.3(0.7)	+16.4(1.1)	+13.6
Soy 1	4.3	206	12.2	255	29.3	25.3(2.9)	294	1.51 (0.11)	-4.7(0.9)	+11.0(1.1)	+11.0
Soy 2	5.1	300	20.0	237	28.5	37.1(1.6)	342	1.32 (0.14)	-5.1(0.9)	+12.7(0.3)	+11.9
Oak - 40%	3.3	142	11.8	237	28.9	n.d.	-	1.62 (0.18)	-5.6(1.9)	+13.4(1.4)	n.d.
Oak - 20%	4.2	166	15.5	207	29.2	n.d.	-	1.57 (0.17)	-6.6(0.6)	+11.8(0.8)	n.d.
Oak - 2%	4.1	172	17.5	174	27.8	n.d.	-	14.6 (2.2)	-6.2(0.7)	+13.1(1.3)	n.d.

^a In vivo CA hydration based on the mean CA_{assay} of the other two tobacco plants.

species (von Caemmerer and Evans, 1991; Evans et al., 1994), although in the case of oak, g_i was higher than the range previously quoted for oak species (0.15, Loreto et al., 1992; 0.08–0.22 $\text{mol m}^{-2} \text{ s}^{-1}$, Rouspard et al., 1996; 0.07–0.08, Hanba et al., 1999).

$\delta^{18}\text{O}$ of Water at the Site of Oxygen Exchange

Estimates of evaporating surface water (δ_e) were based on direct measurements of transpired water vapor (δ_t) applying the isotopic fractionation during evaporation (Eq. 3). The maintenance of constant vapor pressure deficit (VPD) during the complete photosynthetic photon flux density (PPFD) curve kept both δ_t and δ_e constant throughout each experiment (Table I). Determining δ_e in this way from δ_t avoids uncertainties that arise in substituting source water $\delta^{18}\text{O}$ for δ_t in Equation 3, as shown in Table I; although δ_t is at steady state, the absolute value may differ from source water (-4.5‰) by several per mill.

δ_e is assumed to provide a close approximation to $\delta^{18}\text{O}$ of water in the chloroplasts. The proximity of chloroplasts to evaporating surfaces is sufficient to ensure good isotopic mixing between the two. In particular, this assumption would be safe when ^{18}O heterogeneity in the entire leaf water is small. As a precautionary measure, such heterogeneity was evaluated by comparing δ_e with measured bulk leaf water (δ_{LW}) both at the end of each light response experiment (Table I; Fig. 3, white symbols) and across a range of evaporation rates in an independent test (Fig. 3, black symbols). On average, bulk leaf water was lower than δ_e by 2‰ ($\pm 1\%$ in Fig. 3). This phenomenon has been observed extensively (Wang et al., 1998, and refs. therein) and has been partly explained by the inclusion of unenriched vein water, estimated to represent 2% to 5% of total leaf water (Yakir et al., 1989; Flanagan et al., 1991), and/or by a Peclet effect proposed by Farquhar and Lloyd (1993).

The difference between δ_e and δ_{LW} increased with the evaporation rate (Fig. 3, excluding the three

marked data points, from leaves thought not to be at isotopic steady state), which is consistent with a Peclet effect (Flanagan et al., 1991; Farquhar and Lloyd, 1993). In this case, the large advective flux of water through the leaf at higher evaporation rates restricts back-mixing of ^{18}O -enriched water from the evaporation sites with the bulk leaf water. The maximal Peclet effect observed here was 3‰ (excluding marked points), which was much smaller than those reported previously (Flanagan et al., 1991, 1994; Wang et al., 1998). The small Peclet effect in this

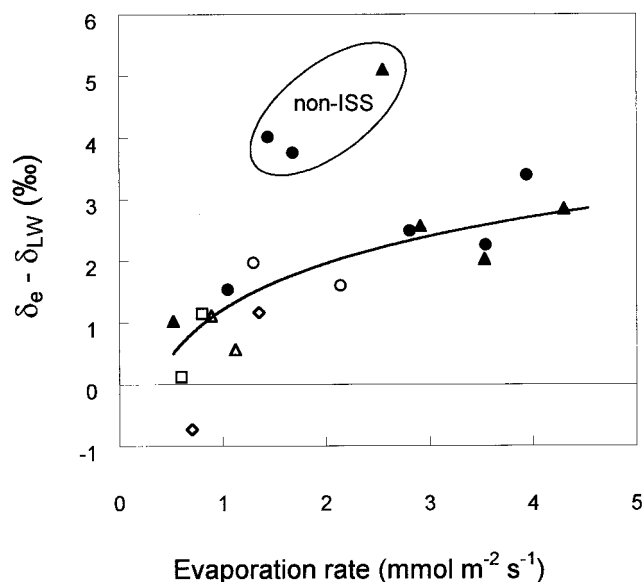


Figure 3. The difference between δ_e from the Craig and Gordon equation and bulk leaf water (δ_{LW}) as a function of evaporation rate (E) for soy (triangles), tobacco (circles), maize (diamonds), and sorghum (squares). White symbols are data from the last measurement of the light response study; black symbols are additional points from the leaf water heterogeneity test. The three marked points excluded from statistical analysis are thought to represent non-steady-state conditions.

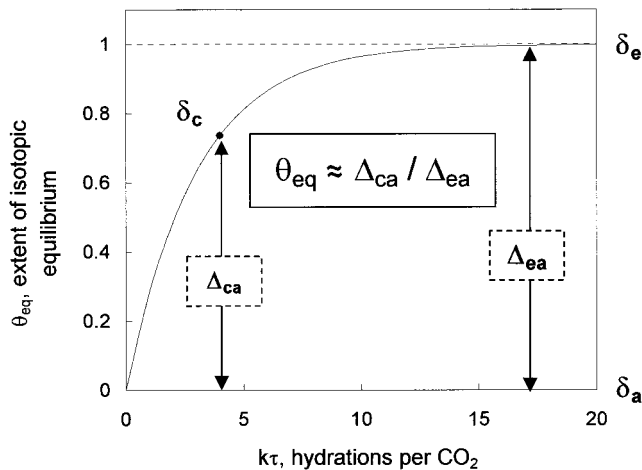


Figure 4. Diagram showing the dynamics of oxygen isotope exchange between atmospheric CO₂ (δ_a) and leaf water (δ_e) and the resulting $\delta^{18}\text{O}$ of CO₂ (δ_c). Isotopic equilibrium (θ_{eq}) from Equation 4, solid line was calculated from the CA activity and CO₂ residence time ($k\tau$), which represents the number of hydrations per CO₂ molecule and is related to $\Delta_{\text{ca}}/\Delta_{\text{ea}}$.

study was probably due to low evaporation rates ($<5 \text{ mmol H}_2\text{O m}^{-2} \text{ s}^{-1}$, Table I). In addition, although not measured here, Peclet effects in oak (K.G. Harwood, D. Yakir, J.S. Gillon, and H. Griffiths, unpublished data) and other woody species (birch and poplar; Roden and Ehleringer, 1999) have been consistently equally low in a wide range of conditions. Therefore, the absence of significant isotopic gradients in leaf water over the whole leaf is a good indication that isotopic gradients are unlikely to occur across the much smaller distances ($<0.01 \text{ mm}$) between evaporating surfaces and chloroplasts.

Extent of CO₂-H₂O Isotopic Equilibrium

We measured CA activity in the experimental plants and used the results to estimate the in vivo extent of isotopic equilibrium between CO₂ and H₂O in the chloroplast. Previously, close to full isotopic equilibrium has been assumed due to the high rates of CA catalysis expected in most plants. We tested this assumption by measuring CA activities under assay conditions and estimating in vivo rates under leaf conditions (at chloroplastic [CO₂] and leaf temperature). Assay rates showed significant variation, with the lowest rates in soy (Table I). Although CA activity for the oak plants used here was not determined, measurements in oak species from previous studies revealed very high CA activity (mean and SD for *Quercus bosserii* -288 ± 36 ; *Quercus robur* -261 ± 25 ; *Quercus pedunculata* $-201 \pm 30 \text{ mmol CO}_2 \text{ m}^{-2} \text{ s}^{-1}$; J.S. Gillon and D. Yakir, unpublished survey data). Further differences were introduced when calculating in vivo CO₂ hydration rates, due to small variabilities in leaf temperature and internal [CO₂] between the experiments. Notably, during a light

response curve, CO₂ hydration rates in vivo did not vary considerably. Most likely, reductions in the calculated CO₂ hydration rate associated with decreased internal [CO₂] at high light were compensated for by increased leaf temperatures and enhancement of catalytic activity.

Using the data on CA activity during leaf gas exchange, we could assess the extent of CO₂-H₂O isotopic equilibrium independently of $\Delta^{18}\text{O}$ measurements. The efficiency of CO₂-H₂O isotopic equilibrium depends upon the product $k\tau$, which is residence time (τ) times the rate constant of CO₂ hydration within the chloroplast (k) (see "Materials and Methods"). Combining with the isotope exchange theory of Mills and Urey (1940) for the CO₂-H₂O reaction, the fractional extent of isotopic equilibrium may be described by θ_{eq} (Eq. 4), so that full equilibrium occurs when $\theta_{\text{eq}} = 1$ (corresponding to $k\tau$ greater than 15; Fig. 4). Thus, as CO₂ (with isotopic signal of δ_a) passes through a leaf, the $\delta^{18}\text{O}$ of CO₂ changes, approaching equilibrium with leaf water represented by δ_e . The $\delta^{18}\text{O}$ value of CO₂ in the chloroplast (δ_c) should lie between δ_a and δ_e at some point depending on θ_{eq} (Fig. 4). This effect has already been demonstrated qualitatively in genetically modified plants with low CA activity, where $\Delta^{18}\text{O}$, and therefore δ_c , were dramatically reduced compared with the values expected at full isotopic equilibrium (δ_e) (Price et al., 1994; Williams et al., 1996).

Calculating $k\tau$ and the corresponding extent of isotopic equilibrium for each data point, we observed more than 95% isotopic equilibrium ($\theta_{\text{eq}} > 0.95$) for tobacco (Fig. 5). The lower CA activity in soy sug-

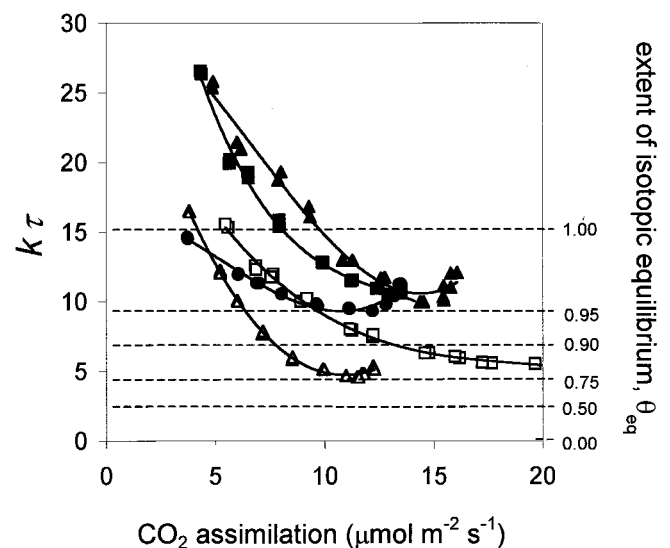


Figure 5. The number of hydration reactions per CO₂ molecule ($k\tau$) calculated from $CA_{\text{leaf}}/F_{\text{in}}$ as a function of the CO₂ assimilation rate. Shown on the second axis is the equivalent extent of isotopic equilibrium from Equation 4, in which full equilibrium ($>99.5\%$) occurs above $k\tau = 15$. White symbols, Soy; black symbols, tobacco (different symbols refer to different light responses). All values for oak were above $k\tau = 15$ because of the assumed high CA rates.

gested that the equilibrium was 75% complete. In the extreme case, potentially high CA activity in oak corresponded to complete isotopic equilibrium throughout the light response, where $k\tau$ was always greater than 15 (data not plotted in Fig. 5). Note that in other plants, including C3 and C4 species, θ_{eq} values were found to span the whole range from 0 to 1 (J.S. Gillon and D. Yakir, unpublished data).

CO₂ Concentration at the Site of Isotopic Equilibrium

Based on the above discussion that δ_c lies between δ_a and δ_e and reflects θ_{eq} , it is possible to show that θ_{eq} is related to Δ_{ca}/Δ_{ea} (Fig. 4), since algebraically:

$$\theta_{eq} = \frac{R_c - R'_c}{R_e - R'_c} = \frac{R_c - R_a \left[1 - \frac{\bar{a}}{\epsilon + 1} \right]}{R_e - R_a \left[1 - \frac{\bar{a}}{\epsilon + 1} \right]} = \frac{\Delta_{ca} + \frac{\bar{a}}{\epsilon + 1}}{\Delta_{ea} + \frac{\bar{a}}{\epsilon + 1}} \quad (5)$$

This describes the ¹⁸O/¹⁶O ratio of CO₂ at the site of oxygen exchange (R_c) relative to that in full equilibrium with leaf water (R_e), and that for non-equilibrated CO₂ inside the leaf, R'_c . The term $R'_c = R_a \cdot (1 - \bar{a}/[\epsilon + 1])$ allows for the variable expression of \bar{a} under non-equilibrium conditions (as in ¹³C discrimination). Thus, $(1 - e^{-k\tau/3}) = \theta_{eq} \approx \Delta_{ca}/\Delta_{ea}$ (Fig 5). We now incorporate the extent of isotopic equilibrium into Eq. 2, and C¹⁸OO discrimination is then given as:

$$\Delta^{18}O = 1,000 \frac{\bar{a} + \epsilon \left[\theta_{eq} \Delta_{ea} - (1 - \theta_{eq}) \frac{\bar{a}}{\epsilon + 1} \right]}{1,000 - \epsilon \left[\theta_{eq} \Delta_{ea} - (1 - \theta_{eq}) \frac{\bar{a}}{\epsilon + 1} \right]} \quad (6)$$

With measured values of $\Delta^{18}O$, Δ_{ea} , and θ_{eq} , we may thus derive ϵ , and hence $c_{c(eff)}$, the effective CO₂ concentration at the site of CO₂-H₂O equilibrium.

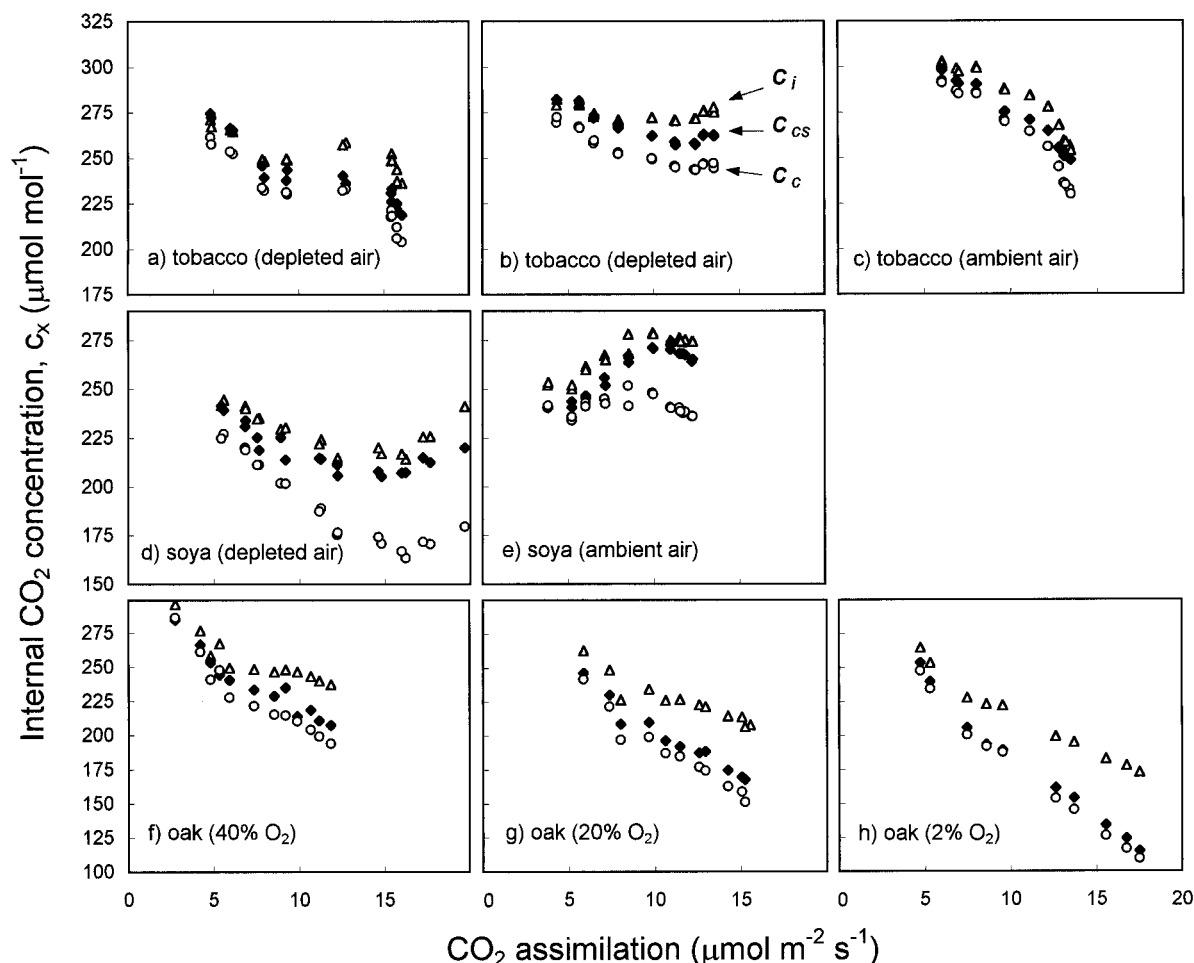


Figure 6. Data shown for all light response curves, showing internal CO₂ concentration ($\mu\text{mol mol}^{-1}$) as a function of CO₂ assimilation rate ($\mu\text{mol m}^{-2} \text{s}^{-1}$). Symbols refer to CO₂ concentration in internal air space (c_i) (from gas exchange measurements, Δ), c_{cs} (from $\Delta^{18}\text{O}$, δ_e , and CA activity; \blacklozenge), and c_c (from $\Delta^{13}\text{C}$; \circ). Species are tobacco (a–c), soy (d–e), and oak (f–h). Light responses in c and e were conducted using ambient $\delta^{18}\text{O}$ CO₂, whereas the rest used CO₂ depleted in ¹⁸O. f through h, Experiments in 40%, 20%, and 2% O₂, respectively.

The $c_{c(\text{eff})}$ values obtained from Equation 6 were always intermediate between c_i (from gas exchange) and c_c (from $\Delta^{13}\text{C}$), as shown in Figure 6. These results were obtained from eight experiments in three species, measured on two separate systems, reducing the likelihood of bias introduced via system or species effects. Typically, all values of internal $[\text{CO}_2]$ dropped at high assimilation rates, as CO_2 demand increased, albeit with variation due to some non-correlated changes in stomatal conductance, particularly for soy. Species differences were evident: $c_{c(\text{eff})}$ was generally closer to c_i in soy, closer to c_c in oak, and intermediate in tobacco.

The values of $c_{c(\text{eff})}$ represent the CO_2 concentration at the effective site of CO_2 - H_2O equilibrium, which we term c_{cs} (Yakir, 1998), indicating that the chloroplast surface is the likely site. This assumes that the limit of CA activity occurs at the chloroplast surface, since the majority of CA resides within the chloroplast (Everson, 1970). These results are consistent with the difference between the effects of Rubisco on $\Delta^{13}\text{C}$ and CA on $\Delta^{18}\text{O}$: although Rubisco and CA show the same distribution within the chloroplast (Anderson et al., 1996), Rubisco removes $^{12}\text{CO}_2$ from the system, creating a ^{13}C gradient between c_c and c_a ; CA only acts to cancel out any ^{18}O gradients in CO_2 throughout the domain of its activity, so that an ^{18}O gradient only exists from the chloroplast surface (c_{cs}) to the atmosphere (c_a) (Fig. 7).

Note that in interpreting $\Delta^{18}\text{O}$, the best-constrained value is δ_e . Consequently, testing the model for $\Delta^{18}\text{O}$ usually involved deriving δ_c values and comparing them with δ_e values. Assuming that we appropriately adjust δ_c for θ_{eq} and correctly estimate c_{cs} , the two values should match. In previous studies, ^{13}C -derived values of c_c were used and the observed difference between δ_e and δ_c was explained in terms of incomplete isotopic equilibrium. The effects of incomplete

equilibrium was addressed in those cases by applying a certain ρ value ($\rho = A/CA_{\text{leaf}}$), which was incorporated within the $\Delta^{18}\text{O}$ model (Farquhar and Lloyd, 1993; Flanagan et al., 1994; Williams and Flanagan, 1996; Williams et al., 1996). Furthermore, the method of c_c determination based on individual $\Delta^{13}\text{C}$ measurements (and not the trend of $\Delta^{13}\text{C}$ across the full range of A) generated a range of c_c values (up to $40 \mu\text{mol mol}^{-1}$), so that co-adjustment of c_c and ρ was required to resolve δ_e versus δ_c differences.

In some cases, estimates of δ_c were as much as 10% below δ_e in both laboratory and field studies (Yakir et al., 1994; Harwood et al., 1998; Wang et al., 1998). Such differences cannot be explained by only considering c_{cs} , and probably imply large heterogeneity in leaf water isotopic composition. Especially in the two latter field studies, Peclet effects may be much larger than observed in this study. It is possible that these discrepancies represent isotopic leaf water heterogeneity between water in the chloroplast and at the evaporating sites. Better characterization of the oxygen exchange site may help future studies of significant leaf water gradients and Peclet effects.

Partitioning Internal CO_2 Conductance

The association of $\Delta^{18}\text{O}$ with the $[\text{CO}_2]$ at the chloroplast surface (c_{cs}) provides us with another reference point in the diffusion pathway from atmosphere to chloroplast in addition to probing c_i via gas exchange (von Caemmerer and Farquhar, 1981) and c_c from $\Delta^{13}\text{C}$ analysis (von Caemmerer and Evans, 1991). From Fick's law of diffusion, CO_2 concentration gradients are related to conductance by the general expression $A = g_x(c_1 - c_2)$. Applying values of c_{cs} , we may partition the total conductance (g_i) into its components before and after the chloroplast surface by plotting A versus $(c_i - c_{cs})$ and versus $(c_{cs} - c_c)$. In each case, the inverse of the gradient refers to cell wall/plasmalemma conductance (g_w) and conductance within the chloroplast (g_{ch}), respectively (Fig. 7), assuming no significant resistance to CO_2 diffusion in the gaseous leaf interior (Evans et al., 1994). Despite a larger error in determining conductances from $\Delta^{18}\text{O}$ compared with $\Delta^{13}\text{C}$, g_w was significantly higher than g_i for both tobacco and soy, and on the borderline of significance for oak (Table II). Comparing the values of g_{ch} relative to g_w , the chloroplast conductance was estimated to be 0.8 (tobacco), 0.3 (soy), and 3.2 (oak) times the wall conductance (g_{ch}/g_w , Table II). The magnitude and species variability of g_{ch} was much lower than previous theoretical estimations, where the wall conductance was thought to be the major limitation to diffusion, such that g_{ch}/g_w was predicted to be from 4.8 (Evans et al., 1994) to 7.4 (Cowan, 1986). The occurrence of low chloroplast conductance was associated with low in vivo CA activities (soy), while potentially high CA activity in oak may be associated with high g_{ch} .

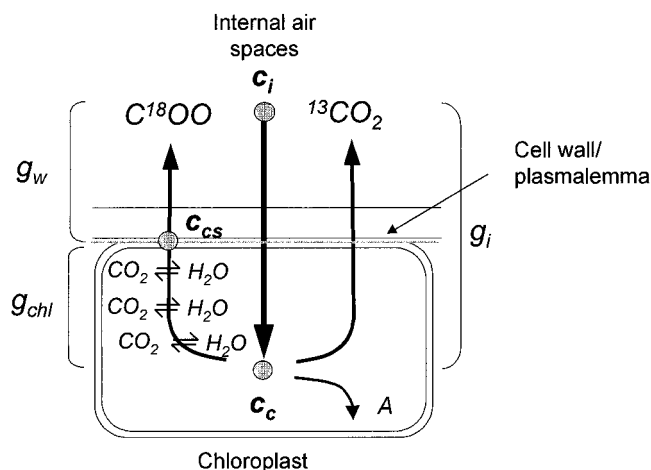


Figure 7. Diagram representing the backflux of CO_2 from sites of CO_2 fixation (c_c) and sites of oxygen exchange (c_{cs}) in the chloroplast, showing the partitioning of total internal conductance (g_i) (relevant to $\Delta^{13}\text{C}$) into chloroplast (g_{ch}) and wall (g_w) conductance (from $\Delta^{18}\text{O}$).

Table II. The breakdown of total leaf CO_2 conductance (g_{leaf}) into its components, stomatal (g_s) (from gas exchange) and internal (g_i) (from $\Delta^{13}\text{C}$, plus error from 95% confidence limits of the slopes)

With $\Delta^{18}\text{O}$, g_i is further partitioned into wall conductance to C_{cs} , g_w , and the residual conductance within the chloroplast, (g_{ch}). All units are $\text{mol CO}_2 \text{ m}^{-2} \text{ s}^{-1}$. The ratio of chloroplast to wall conductance is also shown g_{ch}/g_w . Average CA_{leaf} activity is shown for comparison ($\mu\text{mol m}^{-2} \text{ s}^{-1}$).

Species	g_{leaf}		g_i	g_i		g_{ch}/g_w	CA_{leaf}
	g_s	g_i		g_w	g_{ch}		
Tobacco	0.155	0.224	0.50 (0.12)	1.12 (0.33)	0.90	0.8	623
Soy	0.141	0.253	0.32 (0.05)	1.31 (0.45)	0.42	0.3	318
Oak	0.102	0.166	0.27 (0.09)	0.35 (0.04)	1.13	3.2	2,016 ^a

^a In the absence of direct CA measurements in the oak species used here, CA_{leaf} is estimated from the average CA activity observed other oak species (see text).

Importance of CA-Mediated Diffusion in g_{ch}

It is becoming increasingly evident that CA facilitates diffusion and therefore CO_2 conductance within the chloroplast (Cowan, 1986; Makino et al., 1992; Price et al., 1994; Williams et al., 1996; Sasaki et al., 1998). This may be further supported by the association of CA activity with the relative magnitude of chloroplast conductance in the three species used here (Table II). However, in the past, modification of CA activity has revealed little or no change in photosynthetic rate (Price et al., 1994; Williams et al., 1996), so that the benefit to photosynthesis from CA remains unclear. We now propose that the relative contribution from CA to photosynthetic efficiency may be species dependent and not always clearly apparent. In particular, CA-mediated diffusion may be more important when total internal conductance is low, as is the case for woody species (von Caemmerer and Evans, 1991; Lloyd et al., 1992; Loreto et al., 1992; Syvertsen et al., 1995). In such cases, photosynthetic limitations attributable to low wall conductance (g_w), which occur due to the cellular architecture of sclerophyllous leaves, may be offset by optimizing chloroplast conductance (g_{ch}).

This species effect on CA-mediated g_{ch} is illustrated by estimating CO_2 assimilation as a function of chloroplast conductance (Fig. 8). Assimilation was described as $A = k(c_c - \Gamma^*) - R_{\text{cl}}$, where k and Γ^* are the carboxylation efficiency and compensation point ($k = 0.121$ and 0.073 , $c_i = 208$ and 252 , $\Gamma^* = 40$ and 45 for oak and tobacco, respectively) and $c_c = c_i - A/g_i$. We calculated the change in CO_2 assimilation rate relative to observed values (Fig. 8) due to varying the chloroplast component of internal conductance (while keeping g_w constant, plotted as g_{ch}/g_w in Fig. 8). In oak, with lower wall conductance (high g_{ch}/g_w), the current assimilation rate is 20% higher compared with that which would occur at chloroplast conductance values found in tobacco. Conversely, in tobacco, increasing g_{ch} to the extent found in oak would result in only a 5% increase in A . This example is also consistent with the gas exchange measurements from tobacco plants with genetically reduced

CA activity (Price et al., 1994; Williams et al., 1996). Internal conductance was lower (approximately $0.25 \text{ mol m}^{-2} \text{ s}^{-1}$) in the CA mutant compared with wild-type plants (approximately $0.4 \text{ mol m}^{-2} \text{ s}^{-1}$).

Applying the present ratio of g_{ch}/g_w (0.8) for wild-type tobacco plants, we may calculate the wall conductance for wild-type plants from their $\Delta^{13}\text{C}$ -derived g_i values. Assuming this physical wall conductance is unchanged between wild-type and CA mutant plants (the antisense CA gene should have no other effects on leaf physiology and structure), we estimate a lower value of $g_{\text{ch}}/g_w = 0.5$ for the CA mutant tobacco plants, i.e. the reduction in g_i is due to reduction in g_{ch} only. Indicating the position

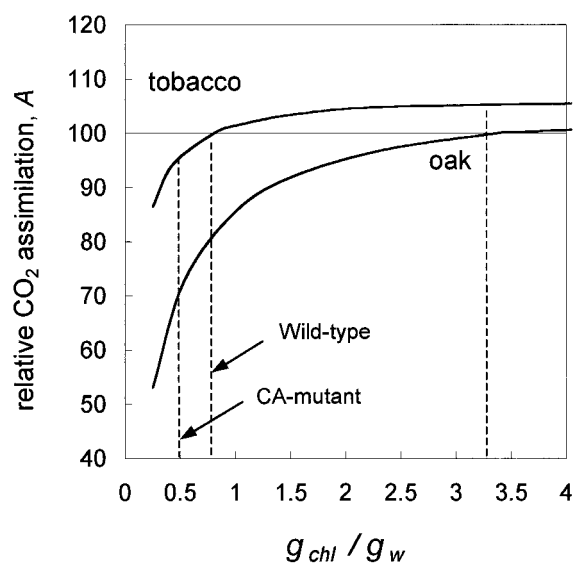


Figure 8. The potential change in CO_2 assimilation rate (A) as a function of g_{ch} (oak and tobacco, solid lines). g_{ch} is normalized relative to a constant wall conductance (g_w) (0.35 and $1.12 \text{ mol m}^{-2} \text{ s}^{-1}$ for oak and tobacco, respectively). The changes in A are expressed relative to measured assimilation rates at actual conductance values, $g_{\text{ch}}/g_w = 0.8$ and 3.2 for tobacco ($A = 12.7 \mu\text{mol mol}^{-1}$) and oak ($A = 13.7 \mu\text{mol mol}^{-1}$), respectively. Also marked is the estimated g_{ch}/g_w (see text) of tobacco mutants lacking CA (Price et al., 1994; Williams et al., 1996), indicating only a small effect on assimilation relative to the wild-type tobacco.

of the CA-mutant plants on Figure 8, we predict only a 5% drop in CO₂ assimilation for the 90% to 95% reduction in CA activity, in agreement with reported results.

Two main points arise from this simple analysis. First, it appears that relative chloroplast conductance is proportional to CA activity across almost three orders of magnitude of CA activity, with a possible minimum at $g_{ch}/g_w = 0.5$, where all residual CO₂ diffusion will be un-facilitated (i.e. no CA effect). This strongly supports the occurrence of CA-mediated diffusion in the chloroplast. Second, although the oak plants used may not be completely representative of woody species, CA activity in woody plants in general may have been optimized over evolutionary time to compensate for low wall conductance (J.S. Gillon and D. Yakir, unpublished data). For example, in a preliminary survey, mean in vivo CA hydration rates were 1,090 and 390 $\mu\text{mol m}^{-2} \text{s}^{-1}$ for trees/shrubs ($n = 16$) and herbaceous species ($n = 12$), respectively, which may correspond to a three-times increase in g_{ch} relative to g_w . By extending such surveys to include conductance estimates (both internal and stomatal), or by manipulating CA activity in species with low internal conductance, the potential importance of CA in photosynthesis may prove to be substantially greater than currently assumed.

MATERIALS AND METHODS

Plant Material

Soy (*Glycine max*), tobacco (*Nicotiana tabacum*), maize (*Zea mays*), and sorghum (*Sorghum bicolor*) were grown

from seed in a greenhouse under ambient light and temperature at Weizmann Institute of Science (WIS). The latter two species were only used in the test of leaf water heterogeneity to increase the scope of the test. Oak seedlings (*Quercus robur*) were provided by the Forestry Commission (UK) in 1991, and kept outside and well-watered in 1-L pots at Moorbank Botanical Gardens (University of Newcastle-upon-Tyne, UK), until required. Measurements were conducted on 6- to 10-week-old plants of soy and tobacco plants and on 5-year-old oak seedlings. Transfer of plant material was several days prior to the experiment to allow acclimatization to laboratory conditions.

System 1 (WIS): Gas Exchange

Figure 9 shows a scheme of the on-line isotope/gas exchange system at WIS. Synthetic air was mixed from N₂, CO₂, and O₂ cylinders using mass flow controllers (MKS Instruments, Andover, MA), and humidified by bubbling a variable portion of the airstream through water at room temperature ($\delta^{18}\text{O} = -4.5\%$, therefore, vapor $\approx -14.5\%$), acidified with two drops of 80% (v/v) H₃PO₄. The airflow was split into reference and analysis airstreams, the latter flow range, 800 to 1,500 mL min⁻¹, was passed to a Parkinson "conifer pod" leaf cuvette (PLC) (model PLC3C, ADC Scientific, Hoddeson, UK), and flow was measured via another mass flow controller. Illumination was from a 250 W projector lamp (GEC, Cleveland), passing through a 3-cm depth of water to reduce infrared radiation. Incident radiation on the leaf was controlled by shading with a predetermined number of Miracloth filters (Calbiochem, San Diego). Absolute CO₂ and H₂O concentration in reference and analysis airstreams were monitored alternately via an infrared gas analyzer (model Li-6262, LI-COR, Lincoln, NE).

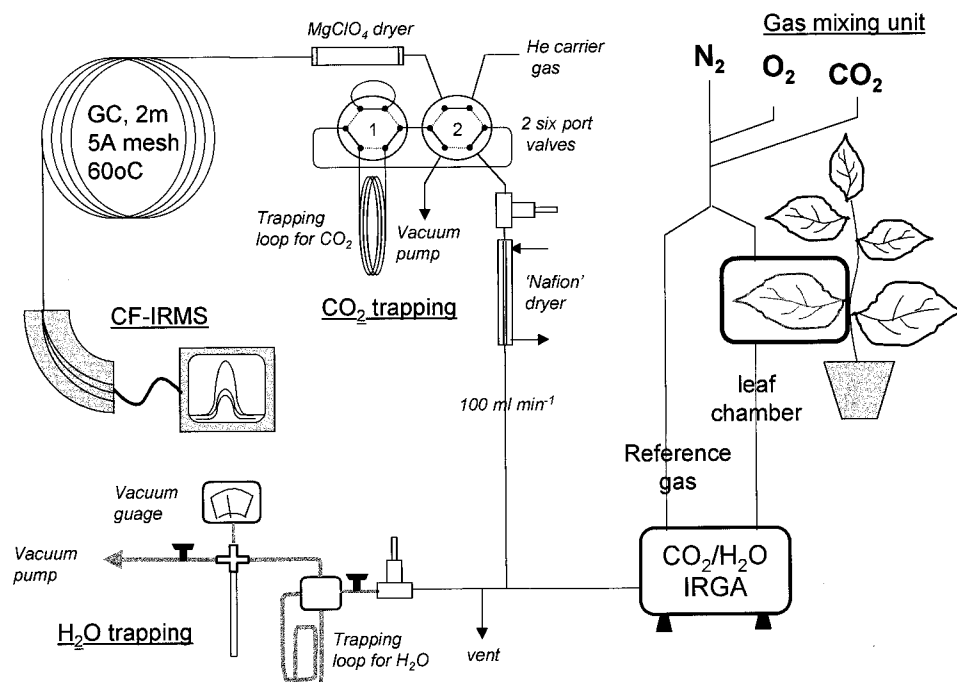


Figure 9. Arrangement of on-line CO₂ trapping and off-line H₂O trapping apparatus for continuous flow CO₂ isotopic analysis, in conjunction with leaf chamber and gas exchange system.

Isotopic Measurement of CO₂

The outflow of the leaf chamber after passing through the infrared gas analyzer (minimum 700 mL min⁻¹) was split, 100 mL min⁻¹ was pumped first through a dryer (Nafion, Perma Pure, Toms River, NJ), and then a sample loop (0.85 mL) was fitted onto a six-port, two-position valve (Valco Instruments, Houston). CO₂ was trapped at liquid N₂ temperatures for 30 s. After warming to room temperature, the sample was swept with helium carrier gas (120 mL min⁻¹; ultrapure, Gordon Gas and Chemicals, Tel Aviv) through a magnesium perchlorate drying trap and a 2-m packed column (sieve 5A, 80/100 mesh, Alltech, Deerfield, IL) at 60°C. The large peaks of N₂ and O₂ that eluted first from the column were diluted via a gas diluter (Micromass, Manchester, UK), followed by the non-diluted sample CO₂. The gas was introduced into the source of a mass spectrometer (OPTIMA, Micromass) via an open split. ¹³C to ¹²C and ¹⁸O to ¹⁶O isotope ratios were measured from the integrated peak areas of masses 44, 45, and 46 normalized against a 30-s CO₂ reference pulse injected prior to each sample. Sample size was standardized by adjusting the cryogenic trapping time according to the CO₂ concentration in the outflow from the leaf chamber. N₂O was assumed to be constant in air (310 nmol mol⁻¹) and absent from "synthetic" air, so δ values were corrected accordingly (Freidli and Siegenthaler, 1988) and expressed in the small delta notation versus Vienna Pee Dee Belemnite (VPDB) for ¹³C and VPDB-CO₂ for ¹⁸O. Precision for repeated sampling of CO₂ was 0.06‰ ($\delta^{13}\text{C}$) and 0.07‰ ($\delta^{18}\text{O}$).

Isotopic Measurement of Water Vapor

The remaining airflow from the leaf chamber was passed at positive pressure to a 0.61-cm o.d. stainless steel vacuum line (pressure <1 × 10⁻³ torr) in which CO₂ and water vapor were trapped from the airstream (3 min at 500 mL min⁻¹) in a coil cooled with liquid N₂. After trapping, the line was evacuated and the trap was heated with a flame, distilling both CO₂ and H₂O into a Pyrex side arm immersed in liquid N₂. After quantitative transfer the pyrex tube was flame sealed. The sample was left for CO₂-H₂O equilibrium at constant temperature (29°C, Labline Instruments, Melrose Park, IL) for 72 h. The CO₂ was then dried in a vacuum line with an ethanol trap at -70°C before isotopic analysis on a dual inlet mass spectrometer (MAT 250, Finnigan-MAT, Bremen, Germany). $\delta^{18}\text{O}$ of water vapor was calculated from that of the CO₂ according to the method of Scrimgeour (1995), correcting for the amount CO₂ and H₂O (calculated from the concentration, flow rate, and time of trapping) and the $\delta^{18}\text{O}$ of the pre-equilibration CO₂, taken from the corresponding measurement of the continuous flow system. Precision of $\delta^{13}\text{C}$ CO₂ and $\delta^{18}\text{O}$ water vapor was 0.04‰ and 0.11‰, respectively.

Experimental Procedure

Light responses were conducted from high to low PPFD (1,200–100 $\mu\text{mol photons m}^{-2} \text{s}^{-1}$, 10 intervals) in 21% O₂. Collections of CO₂ for isotopic analyses were carried out

for 3 min, while water vapor was trapped continuously (i.e. two samples of CO₂ and one of water were analyzed per light level). Photosynthesis measurements were averaged for the collection period. At the end of the experiment, the portion of leaf inside the cuvette was excised and placed in a 15-mL vacuum container (Becton-Dickinson, Rutherford, NJ) for extraction of leaf water. In addition, three leaf discs (1.8 cm²) were cut from the same leaf, and stored in liquid N₂ for subsequent determination of CA activity. The complete light response analysis (approximately 10 determinations) was first conducted with CO₂ relatively depleted in ¹³C and ¹⁸O ($\delta^{13}\text{C} = -30\text{‰}$ and $\delta^{18}\text{O} = -30\text{‰}$) to maximize the precision of measurement. Subsequently, ambient air pumped through a 50-L external buffering volume ($\delta^{13}\text{C} \approx -8\text{‰}$ and $\delta^{18}\text{O} \approx 0\text{‰}$) was used to replicate the experiment. Run-replicate numbers were $n = 3$ for tobacco (two "depleted" and one ambient air) and $n = 2$ for soy (one of each).

System 2 (UNUT)

Photosynthesis measurements and cryogenic trapping of CO₂ and H₂O for the experiments on oak were conducted using the CIRAS-1 (PP Systems, Hitchin, UK) and collection system at UNUT, which is described in Gillon and Griffiths (1997). CO₂ isotopic composition was $\delta^{13}\text{C} = -42\text{‰}$, $\delta^{18}\text{O} = -30\text{‰}$, with $\delta^{18}\text{O}$ water vapor approximately = -18‰. In addition, trapped CO₂ and H₂O were separated via distillation of CO₂ from the mixture using an acetone/liquid N₂ slush at -80°C, as described in Harwood et al. (1998). Precision for dry CO₂ was 0.04‰ ($\delta^{13}\text{C}$) and 0.07‰ ($\delta^{18}\text{O}$). Precision for $\delta^{18}\text{O}$ H₂O determinations was 0.09‰.

Experimental Procedure

A portion of leaf was placed in the chamber and illuminated for 1 to 2 h before beginning measurements. During sampling, CO₂ and water vapor were cryogenically trapped for 15 min from an airstream of 200 mL min⁻¹, during which time photosynthetic parameters were averaged. This was repeated at various PPFDs (500–100 $\mu\text{mol photons m}^{-2} \text{s}^{-1}$, 10–12 steps) to cover the range of CO₂ assimilation from approximately 5 $\mu\text{mol m}^{-2} \text{s}^{-1}$ to saturation, allowing the photosynthetic rate to stabilize between each change in PPFD (approximately 20 min). The leaf-to-air VPD was maintained as constant as possible (approximately 1.5 ± 0.2 kPa) throughout the experiment by drying a portion of the reference airstream with Drierite (W.A. Hammond, Xenia, OH). Reference CO₂ was collected between every three to four samples. The complete light response and isotopic analyses were conducted on the same leaf three times, once each at 2%, 21%, and 35% O₂ to check the influence of photorespiration rate (all other experiments at WIS were conducted at 21% O₂).

Leaf Water Heterogeneity

A separate experiment was carried out at WIS to determine the suitability of the Craig and Gordon model to estimate the $\delta^{18}\text{O}$ of bulk leaf water (δ_{LW}). A leaf was

placed in the cuvette and left for 1 h (the minimum time for the first measurement in the above light response experiments). A dry CO₂ sample from the leaf chamber was first collected in the stainless steel line by passing the airstream through an additional acetone/liquid N₂ trap at -70°C in the vacuum line. This was used to derive the δ¹⁸O CO₂ to be used for equilibration. Next, a water vapor sample from the leaf chamber was collected, as before, and the leaf portion in the cuvette was then excised immediately afterward, and placed in a vacutainer. Finally a reference water vapor sample, bypassing the chamber, was collected (δ¹⁸O ≈ -15‰). This was repeated at different PPF (100–1,500 μmol photons m⁻² s⁻¹) to generate a range of evaporation rates, and repeated for soy, tobacco as well as sorghum and maize, to increase the species range.

Determination of δ¹⁸O Leaf Water

Leaf water was extracted by vacuum distillation at 60°C. δ¹⁸O values were determined by equilibration of 0.2 mL with CO₂ (70 kPa) at 29°C for 24 h, followed by cryogenic separation of a CO₂ aliquot, prior to mass spectrometric analysis. Values were calibrated on the Vienna standard mean oceanic water (VSMOW) scale by simultaneously running internal water standards (WIS H₂O = -4.5‰ VSMOW).

CA Activity

Leaf discs were ground in a pestle and mortar at 4°C with approximately 1 mL of extraction buffer per square centimeter of leaf disc (adapted from Makino et al., 1992). The buffer contained 50 mM 4-(2-hydroxyethyl)-1-piperazineethanesulfonic acid (HEPES)-NaOH (set to pH 8.3) 0.5 mM EDTA, 10 mM dithiothreitol, 10% (v/v) glycerol, and 1% (v/v) Triton X-100 to ensure solubilization of any membrane-bound CA. Extracts were spun at 5,000 rpm for 10 min, and the supernatant was decanted into Eppendorf tubes and frozen at -20°C until assayed. The assay was conducted in a stirred flat-bottomed tube at 2°C. Assay error for the same extract was much smaller than between extracts, so extracts were only assayed once. To 3 mL of assay buffer (20 mM Na-barbitol at pH 8.3), 15 to 50 μL of extract was added, and the assay was started by adding 1 mL of distilled water previously saturated with CO₂ at 0°C. The time for the change from pH 8.3 to 7.3 was recorded. To convert this into a molar rate of CO₂ hydration, the same pH change was titrated with 0.2 N H₂SO₄, assuming the stoichiometry of 1 mole of H⁺ formed for every mole of CO₂ hydrated (Hatch and Burnell, 1990). To calculate the rate of enzymic CO₂ hydration, the rate of a blank assay (i.e. just adding extraction buffer) was subtracted from the rate with leaf extract. The activity (CA_{assay}) was expressed on a leaf area basis (micromoles of CO₂ hydrated per m² per second), representing activity at 2°C and 17.5 mM CO₂. In vivo rates (CA_{leaf}) were calculated at leaf temperature by CA_{leaf} = (17.5 × F·CA_{assay}·[CO₂])/[(17.5 + K_m)([CO₂] + K_m)], where [CO₂] is the concentration at the site of catalysis (from c_{cs}—see “Discussion”—and converted from micromoles per mole to micromolar via Henry’s law), K_m is the concentra-

tion at half maximal activity, taken as 5 mM for dicot CA (data not shown), and the factor *F* was used to correct the rate to leaf temperature, where $F = [(t_{\text{leaf}} - t_{\text{assay}})/10]^{Q_{10}}$, assuming $Q_{10} = 2$ (Hatch and Burnell, 1990).

Coefficient of CO₂ Hydration (*kτ*)

Two main factors control the exchange of ¹⁸O between leaf water and CO₂. During photosynthesis, the gross CO₂ influx rate (*F*_{in}) regulates the residence time (*τ*) of CO₂ in the aqueous leaf medium, while the CA-catalyzed hydration of CO₂ (CA_{leaf}) determines the efficiency of oxygen exchange during that time (Eq. 4). The rate constant for CA (*k*) is equivalent to CA_{leaf}/c_{cs}, and the CO₂ residence time (*τ*) is given by c_{cs}/*F*_{in}. Thus the product, *kτ* = CA_{leaf}/*F*_{in}, relates to the number of hydration reactions per CO₂ molecule. *F*_{in} was determined from the product of external CO₂ concentration (c_a) and total conductance to the site of CO₂-H₂O equilibrium (c_a·g_{leaf}), where g_{leaf} is the combination of boundary (g_b), stomatal (g_s), and internal conductance to c_{cs} (g_w). Using the resistance analogy, g_{leaf} = 1/(1/g_b + 1.6/g_s + 1.6/g_w). Boundary values are quoted in the methods, stomatal values were taken from gas exchange measurements (converting from water to CO₂ via the factor of 1.6), and the internal conductance estimate is described below (and see “Discussion”). Note that *F*_{in} may be also defined as A(ε + 1) from rearranging A = g_{leaf} (c_a - c_{cs}), where ε = c_{cs}/(c_a - c_{cs}).

Photosynthetic Calculations

Photosynthetic parameters were calculated according to the method of von Caemmerer and Farquhar (1981). Due to the influence of oxygen on water vapor determination from infrared gas analyzers (Ludwig et al., 1998), measurements in 2% and 35% O₂ were corrected with an O₂-dependent calibration coefficient (determined from separate tests). Conductance was corrected for the ratio of stomatal density between upper and lower surfaces (K. Parkinson, CIRAS manual, PP Systems, Hitchin, UK), which were measured from epidermal impressions as 0.32, 0.21, and 0.0 for tobacco, soy, and oak, respectively. Boundary layer conductance to H₂O was measured for each species by dipping a leaf in a weak detergent solution, removing excess water, then measuring the evaporation rate in a darkened cuvette (1.1, 0.9 mol m⁻² s⁻¹ for tobacco and soy in a PLC conifer pod, and 3.0 mol m⁻² s⁻¹ for oak in PLC leaf chamber, respectively). Leaf temperature was allowed to vary with PPF, so that maximal *T*_{leaf} at saturating PPF was between 27°C and 29°C for all experiments (minimum *T*_{leaf} = 23°C). *T*_{leaf} was calculated from the energy balance, where radiation and transmission characteristics were either taken from the CIRAS manual for the system at UNUT or measured directly at WIS. The ratio of PPF (Delta-Ohm, Padova, Italy) to total radiation (LI-COR) was determined for the light source, as well as the transmission of the cuvette windows. All of the above parameters can greatly influence the energy budget and hence the calculation of photosynthetic parameters, especially *c_i*, hence we stress that such rigorous determination of

all parameters was essential for interpreting plant isotope discriminations.

$\Delta^{13}\text{C}$ Estimation of c_c

The additional reduction in CO_2 concentration from c_i to the chloroplast (c_c) was estimated from the difference between the simple model and the measured discrimination ($\Delta_i - \Delta_{\text{obs}}$) (Evans et al., 1986) as:

$$\Delta_i - \Delta_{\text{obs}} = \frac{(b' - a_i)}{g_i} \cdot \frac{A}{P_a} \quad (5)$$

where Δ_{obs} is the discrimination measured in Equation 1, $\Delta_i = a + (b' - a) c_i/c_a$ (Farquhar et al., 1982), where c_i and c_a refer to CO_2 concentration in the substomatal cavity and atmosphere, respectively, a is the fractionation during diffusion in air (4.4‰), and b' is the fractionation during carboxylations (29‰); g_i refers to the total internal conductance, a_i is the combined fractionation (+1.8‰) during dissolution (+1.1‰) and diffusion through the liquid phase (+0.7‰). Internal conductance was derived from the gradient of the $\Delta_i - \Delta_{\text{obs}}$ response versus A/c_a measured concurrently with $\Delta^{18}\text{O}$ during the light responses. This method avoids any influence from photorespiration (Gillon and Griffiths, 1997) and uncertainty in b' . Measurements where $A < 8 \mu\text{mol m}^{-2} \text{s}^{-1}$ were excluded to avoid the influence of dark respiration on $\Delta^{13}\text{C}$ (Gillon and Griffiths, 1997).

Statistical Analysis

For the determination of total internal conductance (g_i) (from A/c_a versus $\Delta_i - \Delta_{\text{obs}}$) and wall conductance (g_w) (from A versus $c_i - c_{\text{cs}}$), linear regressions were obtained by the least square method, also deriving 95% confidence limits for slopes, from which the error for each conductance estimate was derived (Sokal and Rohlf, 1981).

ACKNOWLEDGMENTS

We are grateful for the technical support of Emanuela Negreanu and Ruti Yam, and for the reviewers' comments. Received September 27, 1999; accepted December 1, 1999.

LITERATURE CITED

- Anderson LE, Gibbons JT, Wang X (1996) Distribution of ten enzymes of carbon metabolism in pea (*Pisum sativum*). *Int J Plant Sci* **157**: 525–538
- Buhay WM, Edwards TWD, Aravena R (1996) Evaluating kinetic fractionation factors use for ecologic and paleoclimatic reconstruction from oxygen and hydrogen isotope ratios in plant water and cellulose. *Geochim Cosmochim Acta* **60**: 2209–2218
- Ciais P, Denning AS, Tans PP, A BJ, Randall DA, Collatz GJ, Sellers PJ, White JWC, Trolier M, Meijer HAJ, Francey RJ, Monfray P, Heimann M (1997) A three dimensional synthesis study of $\delta^{18}\text{O}$ in atmospheric CO_2 . Part 1: Surface fluxes. *J Geophys Res* **102**: 5873–5883
- Cowan IR (1986) Economics of carbon fixation in higher plants. In TJ Givnish, eds, *On the Economy of Plant Form and Function*. Cambridge University Press, Cambridge, UK, pp 133–170
- Craig H, Gordon HI (1965) Deuterium and oxygen-18 variations in the ocean and marine atmosphere. In E Tongiorgi, eds, *Proceedings of a Conference on Stable Isotopes in Oceanographic Studies and Palaeotemperatures*. Laboratory of Geology and Nuclear Science, Pisa, pp 9–130
- Evans JR, Sharkey TD, Berry JA, Farquhar GD (1986) Carbon isotope discrimination measured concurrently with gas exchange to investigate carbon dioxide diffusion in leaves of higher plants. *Aust J Plant Physiol* **13**: 281–292
- Evans JR, von Caemmerer S, Setchell BA, Hudson GS (1994) The relationship between CO_2 transfer conductance and leaf anatomy in transgenic tobacco with a reduced content of Rubisco. *Aust J Plant Physiol* **21**: 475–495
- Everson RG (1970) Carbonic anhydrase and CO_2 fixation in intact chloroplasts. *Phytochemistry* **9**: 25–32
- Farquhar GD, Lloyd J (1993) Carbon and oxygen isotope effects in the exchange of carbon dioxide between terrestrial plants and the atmosphere. In JR Ehleringer, AE Hall, GD Farquhar, eds, *Stable Isotopes and Plant Carbon-Water Relations*. Academic Press, San Diego, pp 47–70
- Farquhar GD, Lloyd J, Taylor JA, Flanagan LB, Syvertsen JP, Hubick KT, Wong SC, Ehleringer JR (1993) Vegetation effects on the isotope composition of oxygen in atmospheric carbon dioxide. *Nature* **363**: 439–443
- Farquhar GD, O'Leary MH, Berry JA (1982) On the relationship between carbon isotope discrimination and the intercellular carbon dioxide concentration in leaves. *Aust J Plant Physiol* **9**: 121–137
- Flanagan LB, Compstock JP, Ehleringer JR (1991) Comparison of modeled and observed environmental influences on the stable oxygen and hydrogen isotope composition of leaf water in *Phaseolus vulgaris* L. *Plant Physiol* **96**: 588–596
- Flanagan LB, Phillips SL, Ehleringer JR, Lloyd J, Farquhar GD (1994) Effect of changes in leaf water oxygen isotopic composition on discrimination against $\text{C}^{18}\text{O}^{16}\text{O}$ during photosynthetic gas exchange. *Aust J Plant Physiol* **21**: 221–234
- Francey RJ, Tans PP (1987) Latitudinal variation in oxygen-18 of atmospheric CO_2 . *Nature* **327**: 495–497
- Freidli H, Siegenthaler U (1988) Influence of N_2O on isotope analysis in CO_2 and mass-spectrometric determination of N_2O in air samples. *Tellus* **40B**: 129–133
- Gillon JS, Griffiths H (1997) The influence of (photo) respiration on carbon isotope discrimination in plants. *Plant Cell Environ* **20**: 1217–1230
- Gonfiatini R, Gratzu S, Tongiorgi E (1965) Oxygen isotope composition of water in leaves. In *Use of Isotopes and Radiation in Soil-Plant Nutrition Studies*. IAEA, Vienna, pp 405–410
- Hanba YT, Miyazawa S, Terashima I (1999) The influence of leaf thickness on the CO_2 transfer conductance and leaf stable carbon isotope ratio for some evergreen tree species in Japanese warm temperate forests. *Funct Ecol* (in press)

- Harwood KG, Gillon JS, Griffiths H, Broadmeadow MSJ** (1998) Diurnal variation of $\Delta^{13}\text{CO}_2$, $\Delta\text{C}^{18}\text{O}^{16}\text{O}$ and evaporative site enrichment of $\delta\text{H}_2^{18}\text{O}$ in *Piper aduncum* under field conditions in Trinidad. *Plant Cell Environ* **21**: 269–283
- Hatch MD, Burnell JN** (1990) Carbonic anhydrase activity in leaves and its role in the first step of C₄ photosynthesis. *Plant Physiol* **93**: 825–828
- Lloyd J, Syvertsen JP, Kriedemann PE, Farquhar GD** (1992) Low conductances for carbon dioxide diffusion from stomata to the sites of carboxylation in leaves of woody species. *Plant Cell Environ* **15**: 873–899
- Loreto F, Harley PC, Di MG, Sharkey TD** (1992) Estimation of mesophyll conductance to carbon dioxide flux by three different methods. *Plant Physiol* **98**: 1437–1443
- Ludwig M, von Caemmerer S, Price D, Badger M, Furbank RT** (1998) Expression of tobacco carbonic anhydrase in the dicot *Flaveria bidentis* leads to increased leakiness of the bundle sheath and a defective CO₂ concentrating mechanism. *Plant Physiol* **117**: 1071–1081
- Luo Y, Sternberg LSL** (1992) Spatial D/H heterogeneity of leaf water. *Plant Physiol* **99**: 348–350
- Makino A, Sakashita H, Hidema J, Mae T, Ojima K, Osmond B** (1992) Distinctive responses of ribulose-1,5-bisphosphate carboxylase and carbonic anhydrase in wheat leaves to nitrogen nutrition and their possible relationship to CO₂ transfer resistance. *Plant Physiol* **100**: 1737–1743
- Mills GA, Urey HC** (1940) The kinetics of isotopic exchange between carbon dioxide, bicarbonate ion, carbonate ion and water. *J Am Chem Soc* **62**: 1019–1026
- Price D, von Caemmerer S, Evans JR, Yu JW, Lloyd J, Oja V, Kell P, Harrison K, Gallagher A, Badger M** (1994) Specific reduction of chloroplast carbonic anhydrase activity by antisense RNA in transgenic tobacco plants has a minor effect on photosynthetic CO₂ assimilation. *Planta* **193**: 193–331
- Roden JS, Ehleringer JR** (1999) Observations of hydrogen and oxygen isotopes in leaf water confirm the Craig-Gordon model under wide-ranging environmental conditions. *Plant Physiol* **120**: 1165–1173
- Roupsard O, Gross P, Dreyer E** (1996) Limitation of photosynthetic activity by CO₂ availability in the chloroplasts of oak leaves from different species and during drought. *Ann Sci Forest* **53**: 243–254
- Sasaki H, Hirose T, Watanabe Y, Ohsugi R** (1998) Carbonic anhydrase activity and CO₂ transfer resistance in Zn-deficient rice leaves. *Plant Physiol* **118**: 929–934
- Scrimgeour CM** (1995) Measurement of plant and soil water isotope composition by direct equilibration methods. *J Hydrol* **172**: 261–274
- Sokal RR, Rohlf FJ** (1981) *Biometry*, Ed 2. W.H. Freeman, New York
- Syvertsen JP, Lloyd J, McConchie C, Kriedemann PE, Farquhar GD** (1995) On the relationship between leaf anatomy and CO₂ diffusion through the mesophyll of hypostomatous leaves. *Plant Cell Environ* **18**: 149–157
- von Caemmerer S, Evans JR** (1991) Determination of the average partial pressure of carbon dioxide in chloroplasts from leaves of several C₃ plants. *Aust J Plant Physiol* **18**: 287–306
- von Caemmerer S, Farquhar GD** (1981) Some relationships between the biochemistry of photosynthesis and the gas exchange of leaves. *Planta* **153**: 376–387
- Wang XF, Yakir D** (1995) Temporal and spatial variations in the oxygen-18 content of leaf water in different plant species. *Plant Cell Environ* **18**: 1377–1385
- Wang XF, Yakir D, Avishai M** (1998) Non-climatic variations in the oxygen isotopic compositions of plants. *Glob Change Biol* **4**: 835–849
- Williams TG, Flanagan LB** (1996) Effect of changes of water content on photosynthesis, transpiration and discrimination against ¹³CO₂ and C¹⁸O¹⁶O in *Pleurozium* and *Sphagnum*. *Oecologia* **108**: 38–46
- Williams TG, Flanagan LB, Coleman JR** (1996) Photosynthetic gas exchange and discrimination against ¹³CO₂ and C¹⁸O¹⁶O in tobacco plants modified by an antisense construct to have low chloroplastic carbonic anhydrase. *Plant Physiol* **112**: 319–326
- Yakir D** (1998) Oxygen-18 of leaf water: a crossroad for plant-associated isotopic signals. In H Griffiths, eds, *Stable Isotopes and the Integration of Biological, Ecological and Geochemical Cycles*. BIOS Scientific Publishers, Oxford, pp 147–168
- Yakir D, Berry JA, Giles L, Osmond CB** (1994) Isotopic heterogeneity of water in transpiring leaves: identification of the component that controls the $\delta^{18}\text{O}$ of atmospheric O₂ and CO₂. *Plant Cell Environ* **17**: 73–80
- Yakir D, De Niro MJ, Rundel PW** (1989) Isotopic inhomogeneity of leaf water: evidence and implications for the use of isotopic signals transduced by plants. *Geochim Cosmochim Acta* **53**: 2769–2773
- Yakir D, Wang XF** (1996) Estimation of CO₂ and water fluxes between terrestrial vegetation and the atmosphere from isotope measurements. *Nature* **380**: 515–517